Mechanisms for Breakdown of Halomethanes through Reactions with Ground State Cyano Radicals

Pooria Farahani,[a] Satoshi Maeda,[b] Joseph S. Francisco, [c] and Marcus Lundberg*,[a]

Abstract: One route to break down halomethanes is through reactions with radical species. The capability of the Artificial Force Induced Reaction (AFIR) algorithm to efficiently explore a large number of radical reaction pathways has been illustrated for reactions between haloalkanes CX_3Y (X= H,F; Y=Cl,Br) and ground state ($^2\Sigma^+$) cyano radicals (CN). For CH_3Cl + CN 71 stationary points in eight different pathways have been located and, in agreement with experiment, the highest rate constant (10^8 $s^{-1}M^{-1}$ at 298 K) is obtained for hydrogen abstraction. In CH_3Br the rate constants for hydrogen and halogen abstraction are similar (10^9 $s^{-1}M^{-1}$) while replacing hydrogen with fluorine eliminates the hydrogen abstraction route and decreases the rate constants for halogen abstraction by 2-3 orders of magnitude. The detailed mapping of stationary points opens up for accurate calculations of product distributions and the encouraging rate constants motivate future studies with other radicals.

Introduction

Halocarbons have been widely used as refrigerants, aerosol propellants, foam blowing agents, and chemical solvents because they are chemically stable, nonflammable, and relatively nontoxic. Many halocarbons, such as chlorofluorocarbons (CFCs), are relatively inert to reactions with the dominant atmospheric radical, the hydroxyl (OH) radical, and have accumulated in the stratosphere. The main sink for their destruction in the stratosphere is by photolysis, a process that releases halogen atoms, which catalyse the breakdown of stratospheric ozone.[1] For this reason, production of halocarbons has been reduced in accordance with the London amendment of the Montreal Protocol. However, there remain large amounts of chlorofluorocarbons in the atmosphere and a massive stockpile on the Earth's surface.[2] As a consequence there is considerable interest in processes that break down these materials.[3]

To initiate the breakdown process typically requires high temperatures or high-energy photons. Despite being inert to OH radicals, CFCs can react with other radicals.[4] The initial reactions in turn create a number of secondary radical species that undergo further reactions. Accurate models of CFC stability thus require an understanding of reaction pathways for many different atmospheric and combustion radicals.

A promising tool to address this problem is the Artificial Force Induced Reaction (AFIR) algorithm.[5] This is a new computational algorithm that automatically locates stationary points of a bimolecular reaction without requiring any assumptions about the mechanism. With a stepwise application of the algorithm, complete reaction pathways can be calculated, and all possible products can be identified. In previous applications of AFIR on other systems, a large number of pathways were found that had not been considered in manual explorations of the potential energy surfaces.[5-6] To explore how this approach can be used to analyse reactions between haloalkanes and radicals, the AFIR algorithm based on accurate Gaussian-4 (G4) theory,[7] has been applied to the reactions between ground state ($^2\Sigma^+$) cyano radicals (CN) and four different halomethanes (CH_3Cl, CF_3Cl, CH_3Br, and CF_3Br). Chloromethane, CH_3Cl, is the most abundant organohalogen in the atmosphere and large amounts are produced by photoreactions between chlorine in ocean water and biomass from marine algea.[8] Bromomethane, CH_3Br, has due to its ozone depletion potential been phased out as fumigant but ocean marine organisms remain an important source. These two haloalkanes are not inert as the C-H bonds can react with a number of atmospheric species. They are included in the present study to allow for a direct comparison with experimental data and to outline reactivity trends. Chlorotrifluoromethane (CFC-13), CF_3Cl, has largely been phased out, but is due to its long-term stability, still present in the atmosphere. Bromotrifluoromethane, CF_3Br, known as Halon 1301, was widely used in fire extinguishers, but is now also banned. In addition to their effect on the ozone layer, many halomethanes are also powerful greenhouse gases.

Cyano radicals have attracted considerable interest, both in combustion and atmospheric chemistry.[9] These radicals are created from hydrogen cyanide (HCN) or acetonitrile (CH_3CN) released during biomass burning, either through photodissociation or reactions with hydroxyl (OH) or oxygen atom (O) radicals.[10] The reactivity of cyano radicals has been extensively analysed, mainly in systems with unsaturated carbons.[11] These reactions proceed without a barrier in the entrance channel, and often lead to hydrogen elimination,[9] e.g., in the reactions with ethene,[12] pentene,[13] and butadiene.[14] Methyl radical elimination is also observed, e.g., in the reaction with propene.[15] Reactions between cyano radicals and saturated hydrocarbons typically leads to the formation of HCN through hydrogen abstraction.[16] The reactions are barrierless in the entrance channel, except for the reaction with methane where there is a small energy barrier.[17] The mechanistic assignment is

[a] P. Farahani, Dr. M. Lundberg
Department of Chemistry – Ångström Laboratory
Uppsala University
Box 518, SE 751 20, Uppsala, Sweden.
Fax: +46-18-471 36 33
E-mail: marcus.lundberg@kemi.uu.se
[b] Prof. S. Maeda
Department of Chemistry, Faculty of Science
Hokkaido University
Kita-10-jyo-nishi-8-cho-me, Kita-ku, Sapporo, 060-0810, Japan.
[c] Prof. J.S. Francisco
Department of Chemistry
Purdue University
560 Oval Drive, West Lafayette, IN 47907, USA.

Supporting information for this article is given via a link at the end of the document.

supported by the presence of a significant deuterium kinetic isotope effect (KIE) and by theoretical calculations.[17b]

Despite the interest in the chemistry of cyano radicals, little is known about their interactions with haloalkanes. Compared to methane, a number of new reaction routes become available, e.g., halogen abstraction and halogen elimination through direct S_N2-type reactions. In each case, either the carbon or the nitrogen of the cyano radical can react, leading to a large number of different pathways. Data from laser-induced fluorescence spectroscopy exist for one system, the gas-phase reaction between cyano radicals and chlorinated methanes.[18] For CH_3Cl there is an activation energy in the entrance channel (2.2 kcal/mol) and a deuterium isotope effect of 2.3, suggesting that hydrogen abstraction is the dominant entrance channel. The reactions with CH_2Cl_2 and $CHCl_3$ (chloroform) also mainly proceed through hydrogen abstraction.[19]

To discriminate between the different AFIR pathways for the CX_3Y + CN reactions, free-energy barriers are calculated using the G4 composite method,[7] which has an average error in barrier heights of less than 1 kcal/mol.[20] The high accuracy makes it possible to select the preferable pathway based on the relative rate constants in the entrance channels. The results also enable an analysis of how substitutions, e.g., bromine instead of chlorine, and fluorine instead of hydrogen, affect the relative stabilities of different halomethanes.

Results

The CX_3Y + CN reactions go through up to eleven different reaction pathways, each with several minima and transition states (TS). All these stationary points are assigned a number in the AFIR algorithm, and these numbers have been kept as convenient labels. However, they do not signify any particular sequences for the reactions.

Three approximations have been made in the presentation of the results. First, only mechanisms with barriers within 8 kcal/mol of the lowest calculated barrier have been considered. This energy difference corresponds to twice the estimated maximum error. Second, the molecular complex converts a major part of the reaction energy into vibrational excitations. As an example, hydrogen abstraction by cyano radicals mainly leads to vibrational excitation of the C–H bond of hydrogen cyanide.[16b, 21] Third, energy distribution between internal degrees of freedom is faster than energy dissipation. In this approximation, also transition states with relatively large energy differences compared to the preceding minima can be overcome, as long as the energy of the transition state is lower than the barrier in the entrance channel.

The CH_3Cl + CN reaction is explained in detail, including the complete reaction pathways for the relevant entrance channels. The mechanisms for other haloalkanes are described with reference to the CH_3Cl pathways, focusing on the effects on the energies when substituting chlorine for bromine and hydrogen for fluorine.

CH_3Cl + CN

Starting from the separated CH_3Cl and CN fragments, geometry optimization gives three local minima on the electronic energy surface, see Figure 1. The difference between these structures is the relative orientation of the two fragments. However, they are not stable species as the significant loss of entropy (~10 kcal/mol) when a molecular complex is formed from two separate fragments leads to positive free energies for all three.

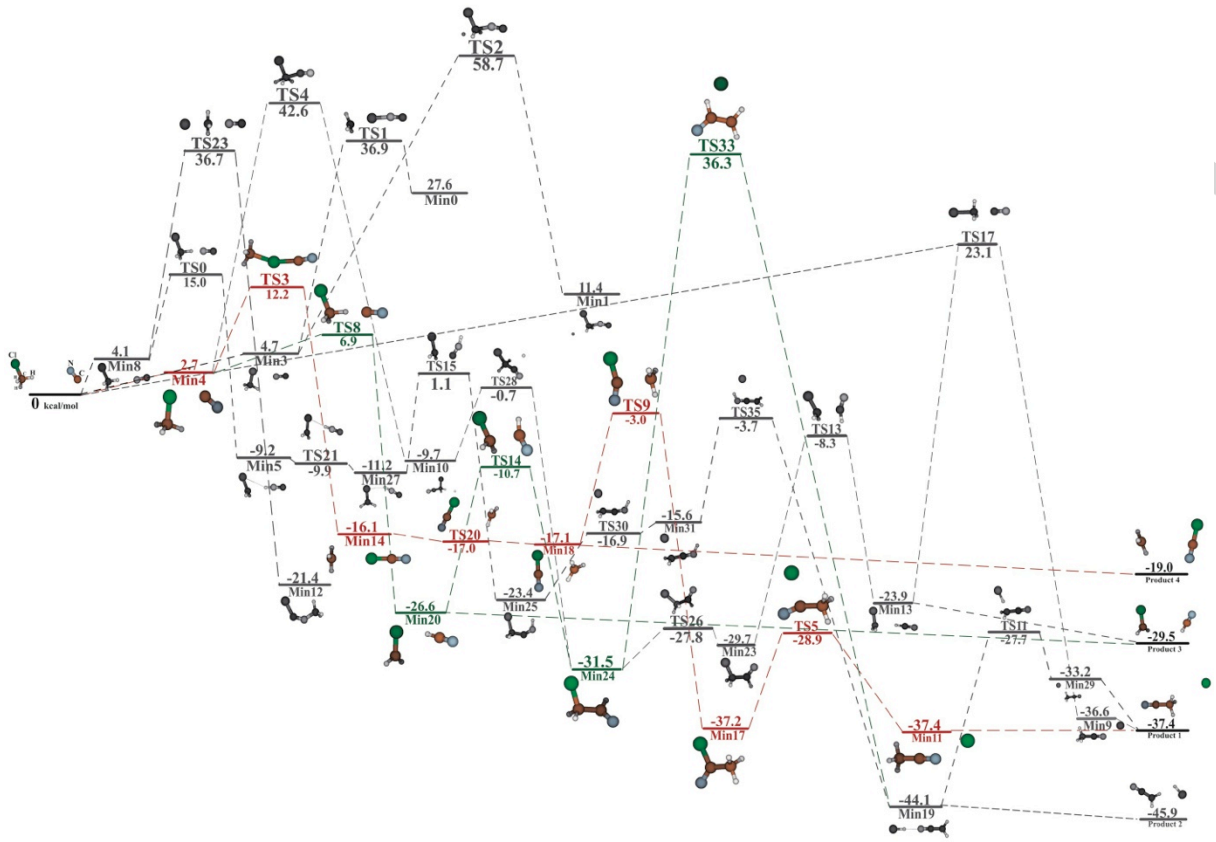

Figure 1. Selected stationary points and reaction pathways for the CH_3Cl + CN reaction obtained from the AFIR algorithm. Relative free energies (in kcal/mol) are calculated using the G4 method. The transition states in the entrance channels are shown in **Figure 2**.

From these three reactant complexes, eight different pathways have been located, see Figure 1. The geometries and relative energies of the transition states in the entrance channels are shown in Figure 2. The lowest free-energy barrier, 6.9 kcal/mol, is obtained for hydrogen abstraction by the cyano carbon (TS8), followed by 12.2 kcal/mol for chlorine abstraction by the cyano carbon (TS3). The corresponding reactions with the cyano nitrogen instead of the carbon have higher barriers, 15.0 kcal/mol for hydrogen abstraction (TS0) and 36.9 kcal/mol for chlorine abstraction (TS1). Two S_N2 transition states with a chlorine radical as the leaving group are also located, one with carbon as the nucleophile (TS17 at 23.1 kcal/mol), and one with nitrogen (TS23 at 36.7 kcal/mol). To complete the list of different pathways, there are two transition states with hydrogen as the leaving group, one for carbon attack (TS4 at 42.6 kcal/mol) and one for nitrogen attack (TS2 at 58.7 kcal/mol).

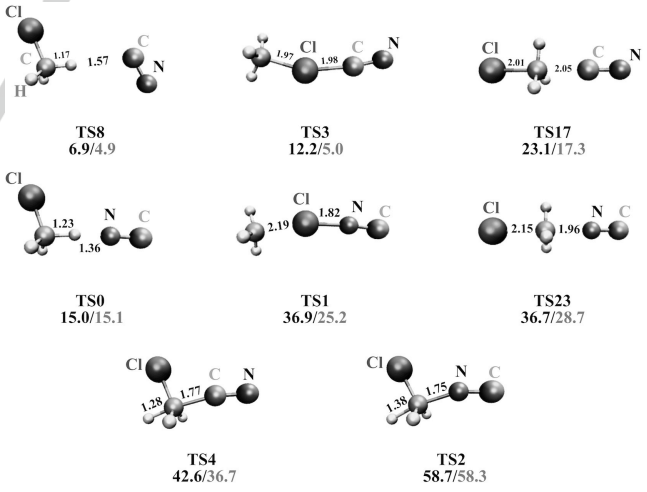

Figure 2. TS structures for the entrance channels of the CH_3Cl + CN system with distances in Å. TS 0, TS3 and TS8 are optimized using QCISD/GTBas3, while the other TS structures are optimized using B3LYP/GTBas3. Free-energy barriers (in kcal/mol) are calculated using the G4 method. The corresponding values for CH_3Br + CN are shown after the forward slash.

Due to the large differences in barrier heights, only the two pathways with the lowest transition state barriers, hydrogen and chlorine abstraction by the cyano carbon, require a more detailed description. The TS for hydrogen abstraction by the cyano carbon (TS8 - green path in Figure 1) is almost collinear with an angle of 178°, similar to what has been suggested for hydrogen abstraction from chloroform ($CHCl_3$).[19b] Hydrogen abstraction leads to formation of hydrogen cyanide and a chloromethyl radical (CH_2Cl) (Min20). This CH_2Cl + HCN intermediate shows a typical halogen bonding pattern with the hydrogen perpendicular to the C–Cl bond.[22] These two fragments can then either dissociate (Product 3 at -29.5 kcal/mol) or combine to form the CH_2ClCHN radical (Min24 at -31.5 kcal/mol), see Figure 1. From CH_2ClCHN there are two pathways, but both of them have exceedingly high barriers. Breaking the C–Cl bond (TS33) has a barrier of 36.3 kcal/mol, while the second pathway eventually leads to the same TS as in the direct S_N2 reaction (TS17), which has a barrier of 23.1 kcal/mol. The hydrogen abstraction pathway thus does not proceed past the CH_2ClCHN intermediate.

Chlorine abstraction by carbon (TS3 - red path in Figure 1) leads to formation of a methyl radical (CH_3) and cyanogen chloride (ClCN) (Min14). These fragments can either dissociate (Product 4 at -19.0 kcal/mol), or the methyl group can, after some rearrangement, attack the carbon of the cyanogen chloride (TS9 at -3.0 kcal/mol) giving methyl cyanogen chloride (CH_3CClN) (Min17). From this intermediate the C–Cl bond breaks (TS5 at -28.9 kcal/mol), leading to acetonitrile and chlorine radical (Min11). They either dissociate (Product 1 at -37.4 kcal/mol) or react through hydrogen abstraction (TS11 at -27.7 kcal/mol) to form the stable cyanomethyl radical (CH_2CN) and hydrogen chloride (HCl) product (Product 2 at -45.9 kcal/mol).

CH_3Br + CN

Substituting chlorine for bromine is not expected to have any major effects on the reaction pathways. The stationary points of the bromomethane system, see Figure S1 in the Supporting Information, were therefore located starting from the stationary points of the chloromethane system. In almost all cases, similar stationary points could be located, although with important differences in relative energies.

Optimization leads to the same three reactant complexes as in CH_3Cl. The main difference is that one of the complexes, (Min4) has a negative free energy (-0.3 kcal/mol) and could possibly be a metastable species. From these minima, eight different TS have been located, just as for chloromethane. The barrier heights are given in Figure 2 and the TS structures are given in Figure S2. Hydrogen abstraction by the carbon of the cyano radical (TS8) has a barrier of only 4.9 kcal/mol, 2 kcal/mol lower than the corresponding barrier for CH_3Cl. As expected, the effect substitution effect is larger for halogen abstraction with a barrier of 5.0 kcal/mol for bromine, a decrease of 7.2 kcal/mol compared to chlorine. The direct S_N2 reactions are also facilitated by Br substitution, but they are still higher than the abstraction reactions by more than 12 kcal/mol. In all cases, reactions with the cyano nitrogen have higher barriers, and hydrogen elimination reactions remain high in energy (>36 kcal/mol).

The two pathways with the lowest barriers in the entrance channel are the same in bromomethane and chloromethane, hydrogen (TS8) and halogen (TS3) abstraction by the cyano carbon. Hydrogen abstraction (green path in Figure S1) leads to a similar pathway as in the CH_3Cl system, with formation of HCN and a bromomethyl radical (CH_2Br) (Min20), which can either dissociate (Product 3 at -27.6 kcal/mol) or combine to form the CH_2BrCHN radical (Min24 at -31.6 kcal/mol). From CH_2BrCHN there are no low-barrier pathways, with TS energies of 25.4 kcal/mol and 17.3 kcal/mol for the reactions leading to bromine or hydrogen bromide products.

An important difference between CH_3Cl and CH_3Br is that the barrier for bromine abstraction (5.0 kcal/mol) is similar to the barrier for hydrogen abstraction (4.9 kcal/mol). This pathway (red path in Figure S1) initially leads to formation of a methyl radical and cyanogen bromide (BrCN) (Min 14). This complex can then dissociate (Product 4 at -20.5 kcal/mol) or form a C–C bond (TS9) and make methyl cyanogen bromide CH_3CBrN (Min17). From here there is a low barrier to reach the acetonitrile and bromine radical product (Product 1 at -50.6 kcal/mol).

CF_3Cl + CN

For CH_3Cl the lowest TS barrier was obtained for hydrogen abstraction by the cyano carbon. In chlorotrifluoromethane (CF_3Cl), the corresponding fluorine abstraction pathways are blocked due to the inert C–F bonds. As this significantly changes the possible reaction pathways, a separate AFIR exploration was performed for CF_3Cl + CN. Reaction pathways with high barriers in the entrance channel were not pursued further, and the potential energy diagram for the CF_3Cl system, see Figure 3, therefore has fewer stationary points than the corresponding diagram for CH_3Cl + CN.

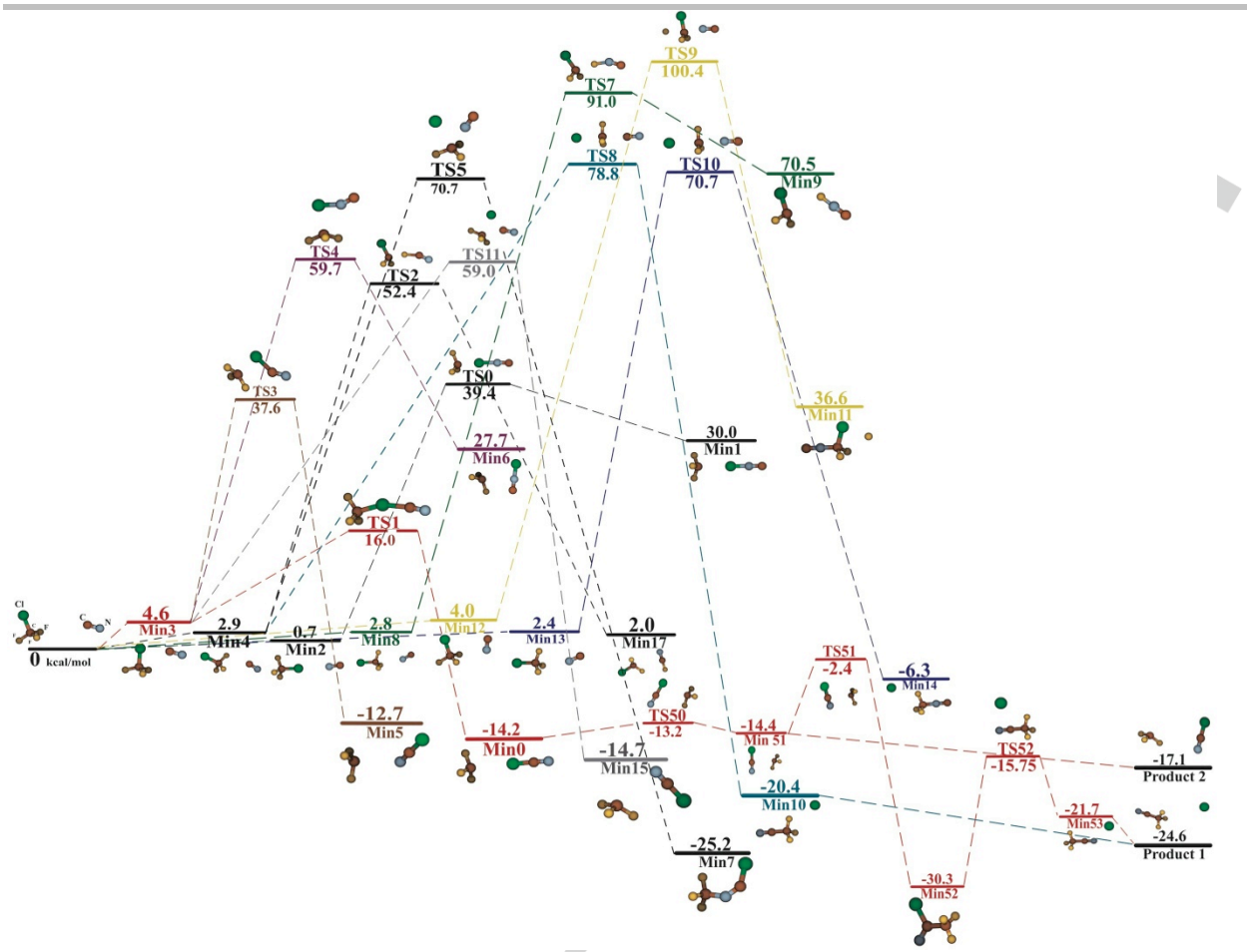

Figure 3. Selected stationary points and reaction pathways for the CF_3Cl + CN reaction obtained from the AFIR algorithm. Relative free energies (in kcal/mol) are calculated using the G4 method. The transition states in the entrance channels are shown in **Figure 4**.

A comparison between the potential energy surfaces of CH_3Cl and CF_3Cl shows significant differences, especially with regard to the barrier heights. Starting from the separated reactants, there are seven minima on the electronic energy surface with different positions of the cyano radical relative to CF_3Cl. From these reactant complexes, twelve different transition states can be located, but most of them have exceedingly high barriers and do not represent viable reaction pathways. Six representative transition states, i.e., the lowest barriers for fluorine abstraction, chlorine abstraction and direct S_N2 reactions are shown in Figure 4. As expected, the barriers for fluorine abstraction with either carbon or nitrogen (TS2 and TS7) are very high, 52.4 and 91.0 kcal/mol respectively. Also the direct S_N2 reactions with chlorine as the leaving group have high barriers, 70.7 kcal/mol with nitrogen as the nucleophile and 78.8 kcal/mol with carbon. This corresponds to significant increases in barrier heights compared to the CH_3Cl reaction even though the fluorine atoms are not directly involved in the reaction. A more detailed analysis of the substitution effects on the S_N2 barriers is given in the Supporting Information.

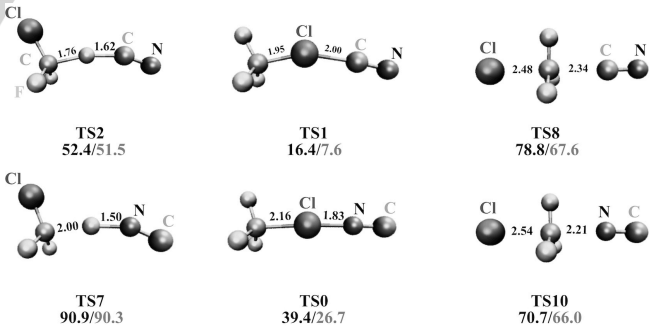

Figure 4. Selected TS structures for the entrance channels of the CF_3Cl + CN system with distances in Ångström. Structures are optimized using B3LYP/GTBas3, except TS1 that is optimized with QCISD/GTBas3. Free-energy barriers (in kcal/mol) are calculated using the G4 method. The corresponding values for CF_3Br + CN are shown after the forward slash.

The high barriers for these reaction pathways leave only one possibility, direct chlorine abstraction. The lowest barrier (16.0 kcal/mol) is obtained for the reaction with the cyano carbon (TS1), while the reaction with the cyano nitrogen (TS0) has significantly

higher barrier (39.5 kcal/mol). Chlorine abstraction by the cyano carbon (red path in Figure 3) gives a similar pathway as for CH_3Cl, this time leading to a trifluoromethyl radical (CF_3) and ClCN complex (Min0). This complex can either dissociate (Product 2), or go through C–C bond formation (TS51 at -2.4 kcal/mol) to form CF_3CCIN (Min52 at -30.3 kcal/mol). From here, breaking the C–Cl bond would give trifluoroacetonitrile (CF_3CN) and a chlorine radical (Product 1 at -24.6 kcal/mol), but the separated products are 5.7 kcal/mol less stable than CF_3CCIN and the reaction does not proceed further. This is different from the CH_3Cl system where the energy decreases by formation of the chlorine radical, and even lower energy could be obtained by the formation of hydrogen chloride.

CF_3Br + CN

The reaction pathways for the CF_3Br system are expected to be similar to those of the CF_3Cl system, and stationary points of the CF_3Br + CN reaction, see Figure S3, were therefore optimized starting from the corresponding points of the chlorine system. Selected free-energy barriers in the entrance channel are given in Figure 4 and TS structures are given in Figure S4. As both fluorine abstraction and S_N2 reactions have very high barriers, the only viable pathways are bromine abstraction. As for the other systems, the barrier is much lower for a reaction with the cyano carbon (TS1 at 6.8 kcal/mol) compared to a reaction with the cyano nitrogen (TS0 at 26.7 kcal/mol), see Figure 4. The major difference between CF_3Cl and CF_3Br is that the reaction barrier for halogen abstraction is significantly lower (by 9.2 kcal/mol) for the latter system. The bromine-containing system is therefore much more reactive. In addition to TS1, there are other pathways for bromine abstraction by the cyano carbon, leading to different orientations of the CF_3 + BrCN intermediates, but they have relatively high barriers (21-50 kcal/mol) and should not be contributing to the reactivity.

Bromine abstraction leads to a similar pathway as in CF_3Cl. The first step is formation of cyanogen bromide (BrCN) and a trifluoromethyl radical (Min0), from which the two alternatives are dissociation (Product 2 at -21.6 kcal/mol) or formation of a CF_3CNBr intermediate (Min52 at -33.9 kcal/mol). From this intermediate, the C–Br bond easily breaks (TS52 at -27.2 kcal/mol), leading to the stable CF_3CN + Br product (-40.7 kcal/mol).

Discussion

The AFIR algorithm shows the considerable complexity of the reactions between haloalkanes and cyano radicals. Fortunately, some of that complexity can be resolved from the reaction barriers in the different entrance channels. Important observations are that direct S_N2 reactions are not favourable and that cyano nitrogen attack is less favourable than carbon attack. The main reaction pathways are therefore hydrogen and halogen abstraction by the cyano carbon. These observations can be explained by the electronic structure of the cyano radical.

All calculations have been made with the cyano radical in the $^2\Sigma^+$ ground state. The $^2\Pi$ and $^2\Sigma^+$ excited states are formed by radiation with shorter wavelength,[23] and appear at higher levels of the atmosphere. In the ground state the lowest unoccupied molecular orbital (LUMO) for the β electrons is a σ_g bonding orbital of a_1 symmetry with dominant carbon character, see Figure 5. This orbital is the third of a set of four σ orbitals with contributions from the C and N 2s, $2p_z$ orbitals, see Figure S5. The carbon atomic orbitals are higher in energy than those of nitrogen, and could be expected to contribute more to antibonding than bonding orbitals. However, because nitrogen mainly contributes to the two lowest orbitals of σ symmetry the two higher-energy orbitals σ orbital are carbon centered. With CCSD the Mulliken spin population of carbon is 0.91, in agreement with the Lewis structure, and carbon carries a partial positive charge (0.22). The calculated dipole moment is 1.56 D, slightly larger than the experimental value of 1.45±0.08 D.[24]

To test the effect of static correlation, the properties of the CN ground state were also calculated using complete active space self-consistent field (CASSCF) with nine electrons in eight valence orbitals, see Figure S5. The active natural orbital with occupation number close to one has 92 % carbon contribution. This gives a Mulliken spin population for carbon of 0.91, in good agreement with the CCSD results.

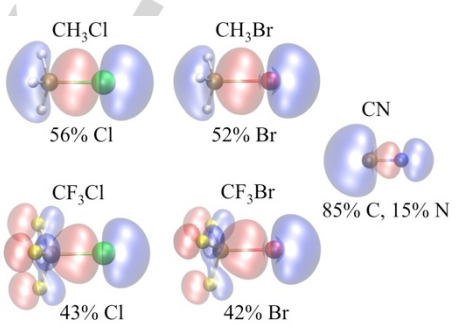

Figure 5. Frontier orbitals calculated using the CCSD/aug-cc-pvtz generalized density for CX_3Y and RO-M062X/aug-cc-pvtz for CN. The orbitals are the highest orbitals of a_1 symmetry (HOMO-2) of CX_3Y and the β LUMO of the cyano radical.

S_N2 reactions with cyanide anions as nucleophiles and chloride or bromide as leaving groups are expected to proceed with low barriers. The high barriers for the direct S_N2 reactions with cyano radicals are explained by the fact that the cyano radical, in contrast to the cyanide anion, is a very poor nucleophile. This is due to the hole in the low-lying σ orbital, which leads to a very high electron affinity.

The higher reactivity of the cyano carbon compared to the cyano nitrogen can be attributed to the predominant carbon character of the β LUMO, and that nitrogen attack products, e.g., isocyanide, are less stable than those formed after carbon attack, e.g., hydrogen cyanide. This is consistent with observations that isocyanide is not formed in reactions with cyano radicals.[16a] The dipole moment of the cyano radical leads to electrostatic effects that can favour either carbon or nitrogen depending on the charge distribution of the substrate. However, these effects do not lead to a lower barrier for nitrogen attack for any of the abstraction reactions.

In all systems the low-barrier pathways are either hydrogen or halogen abstraction by the cyano carbon, see **Scheme 1**. The

different contributions to the free-energy barriers ($\Delta G^{\ddagger}$) of these reactions are analysed in Table 1. The loss of translational entropy when combining two species leads to large entropy contributions ($-T\Delta S^{\ddagger}$) to the barrier height (7.5-8.4 kcal/mol), but the effects are similar for all reactions. One consequence is that conclusions drawn about differences in reactivity from free-energy values calculated at 298.15 K should be valid over a wide temperature range. The enthalpy corrections ($\Delta H^{\ddagger}_{corr}$), dominated by contributions from the zero-point energy, lower the barriers for hydrogen abstraction by 2-3 kcal/mol for all systems but have relatively small effects on halogen abstraction. The major differences between the barrier heights after substitution thus come from differences in electronic energy ($\Delta E^{\ddagger}_{el}$).

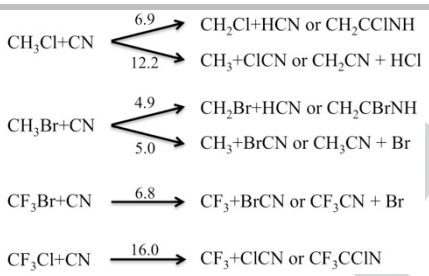

Scheme 1. Summary of preferred reaction mechanisms, barrier heights (in kcal/mol) and possible products for the reactions between halomethanes CX_3Y (X= H,F; Y=Cl,Br) and cyano radicals.

Table 1. Contributions to the free-energy barriers ($\Delta G^{\ddagger}$) of abstraction reactions, rate constants (k), bond dissociation energies (BDE) and relative free energies of the product (ΔG). All energies are in kcal/mol. Electronic energies are calculated using the G4 method with thermal and free-energy contributions calculated using QCISD/GTBas3. Rate constants are calculated using TST with Wigner tunneling corrections

Reaction	$\Delta E^{\ddagger}_{el}$	$\Delta H^{\ddagger}_{corr}$	$-T\Delta S^{\ddagger}$	$\Delta G^{\ddagger}$	k ($s^{1}M^{-1}$)	BDE	ΔG
Hydrogen abstraction							
CH_3Cl	1.2	-2.6	8.4	6.9	7.3×10^{7}	97.0	-26.6
CH_3Br	-0.8	-2.2	8.4	4.9	2.0×10^{9}	98.4	-24.6
Chlorine abstraction							
CH_3Cl	4.8	-0.6	8.0	12.2	8.1×10^{5}	81.5	-16.1
CF_3Cl	8.5	0.1	7.5	16.0	1.4×10^{1}	85.8	-14.2
Bromine abstraction							
CH_3Br	-3.0	-0.3	8.4	5.0	1.4×10^{9}	68.2	-16.0
CF_3Br	-1.5	0.3	8.0	6.8	6.4×10^{7}	74.6	-16.7

Hydrogen and halogen abstraction, i.e., formation of new H–C or Cl–C σ-bonds, occur by attack of the CN β LUMO on the highest CX_3Y occupied orbital of a_1 symmetry, a bonding orbital between both C–X and C–Y, see Figure 5. This is not the highest occupied molecular orbital (HOMO), but HOMO-2, lower in energy than the two halogen (Cl,Br) $p_{x,y}$ orbitals of *e* symmetry, see Figure S6. Calculations of polarizability and Fukui index for radical attack therefore primarily show the properties of these orbitals, instead of those involved in the abstraction reactions.

For CH_3Cl + CN the lowest barrier (6.9 kcal/mol) is observed for hydrogen abstraction by the cyano carbon and the second-order rate constant (*k*) is 7.3×10^{7} $s^{1}M^{-1}$. The activation energy calculated relative to the separated reactants is 1.2 kcal/mol and the corresponding value compared to the preceding reactant complex (Min4) is 2.5 kcal/mol, which should be compared to an experimental activation energy of 2.2 kcal/mol.[18] The deuterium KIE for hydrogen abstraction is calculated to be 5.8, a large discrepancy compared to the experimental value of 2.3, but this can probably be attributed to difficulties of calculating the KIE of an entropy-dominated barrier by standard TST, as previously shown for CH_4 + CN.[17b] The barrier for chlorine abstraction (12.2 kcal/mol) is also relatively low, but the 5.3 kcal/mol difference suggests that hydrogen abstraction should be the dominant pathway. This assignment is in good agreement with other studies of chloromethanes, both in solvent and gas phase.[18-19]

In CF_3Cl there is a clear preference for chlorine abstraction, but the barrier is relatively high, 16.0 kcal/mol, giving a rate constant of 14 $s^{1}M^{-1}$. The lower rate constant is partly due to a 3.8-kcal/mol increase in the free-energy barrier compared to chlorine abstraction in CH_3Cl (3.7 kcal/mol in electronic energy).

In valence bond theory, lower reactivity towards radical abstraction is rationalized using three factors, a higher energy gap in the reactant, directly proportional to the bond dissociation energy (BDE), a less favourable reaction energy (ΔG), and a smaller resonance energy in the TS.[25] The first two of these factors are listed in Table 1. Fluorine substitution increases the C–Cl bond strength by 4 kcal/mol and decreases the exothermicity by 2 kcal/mol, see Table 1. The TS resonance energy depends on the overlap between the reactant and product wavefunctions. In CH_3Cl the major contributions to the frontier orbital come from C $2p_z$ (31%) and Cl $3p_z$ (56%), with only minor contributions (<5%) from other components, see Table 2. In the fluorinated system, the fluorine 2p orbitals contribute strongly to the frontier orbital (33%). These contributions lower the orbital energy, see Table 2, which decreases its electron donor capability. At the same time, the Cl contribution decreases from 56 to 43%, which decreases the overlap with the CN β LUMO during the Cl abstraction reaction, and therefore the resonance energy.

Table 2. Orbital compositions of the highest occupied molecular orbitals of a_1 symmetry calculated from the CCSD/aug-cc-pvtz generalized density. Contributions from polarization functions are not included.

System	C s	C p	H/F s	F p	Cl/Br s	Cl/Br p	Energy (eV)
CH_3Cl	0.8	31.3	3.7	-	3.9	56.4	-14.82
CH_3Br	0.0	35.1	2.4	-	5.2	52.4	-13.80
CF_3Cl	2.3	11.2	0.7	32.6	4.0	43.3	-16.17
CF_3Br	5.2	14.1	0.4	27.2	5.4	41.5	-15.13

The relative barrier heights could also be affected by electrostatic interactions. In CH_3Cl the chlorine atom has a partial charge of -0.12, see Table 3, and this negative charge is expected to lower the barrier for attack by the positive carbon of the cyanide radical. In CF_3Cl the high electron affinity of fluorine changes the chlorine charge to -0.04, which makes carbon attack electrostatically less favourable. The barrier for attack by the negative nitrogen should be favoured by the same change in partial charges, but this barrier increases by 2.5 kcal/mol with fluorine substitution. The electrostatic effect can therefore only be a minor contribution to the changes in barrier heights in CF_3Cl compared to CH_3Cl.

Table 3. ESP charges calculated using the CCSD/aug-cc-pvtz generalized density.

System	C	H	F	Cl
CH_3Cl	-0.48	0.20	-	-0.12
CH_3Br	-0.63	0.24	-	-
CF_3Cl	0.22	-	-0.07	-0.02
CF_3Br	0.19	-	-0.06	-

Substituting chlorine for bromine leads to significantly lower barriers. As an example, direct halogen abstraction decreases from 12.2 kcal/mol in CH_3Cl to 5.0 kcal/mol in CH_3Br, making it competitive with hydrogen abstraction (4.9 kcal/mol). This is consistent with observations for halomethanes and oxygen radical anions, where reactions with bromine are competitive while chlorine reactions are not.[26] The difference in barrier height between hydrogen and halogen abstraction is not large enough to discriminate between the two mechanisms, but the rate constant is high in any case (2.0×10^9 s^1M^{-1} for hydrogen abstraction).

In CF_3Br, where Br abstraction is the only viable pathway, the barrier is 6.8 kcal/mol and the rate constant 6.4×10^7 s^1M^{-1}. The effect of fluorine substitution is an increase in the bromine abstraction barrier by 1.8 kcal/mol (1.5 kcal/mol in electronic energy), the same trend as for the Cl systems. Fluorination increases the strength of the C–Br bond by 6 kcal/mol because the contributions from the F 2p orbitals significant stabilize the σ-bonding orbital. At the same time, the amount of Br in the frontier orbital decreases from 52 to 42 %. Smaller overlap and larger energy difference compared to the CN LUMO leads to an increase in the barrier height. Electrostatic effects, from a change in the partial charge of Br from -0.09 to 0.00, are again expected to be small because the increase in barrier height is similar for attack by the positive carbon and the negative nitrogen, 1.8 and 1.5 kcal/mol respectively.

The trends for the rate constants follow chemical intuition, but they have not been previously quantified. The reaction pathways after the initial abstraction reactions are also completely new. For all systems, the initial abstraction reaction leads to formation of two new fragments; a radical species (CH_2Cl, CH_2Br, CH_3, or CF_3) and a hydrogen or halogen cyanide. These two fragments can either dissociate to form separate products, or they can reach lower free energies by a rebound mechanism. The product distribution depends on the ratio between these two alternatives, and although this ratio cannot be calculated from the AFIR results, the detailed explorations of the potential energy surfaces form starting points for calculations of the detailed reaction dynamics.

If the reactions proceed by the rebound mechanism, which has a low barrier in all systems, it would lead to a wide variety of different products. The hydrogen abstraction pathway in both CH_3Cl and CH_3Br would lead to formation of a metastable CH_2YCNH (Y=Cl,Br) intermediate, from which all forward reactions have prohibitively high barriers. Further reaction thus requires either photodissociation or a collision with another atmospheric molecule. The most stable products in the halogen abstraction pathways of CH_3Cl and CH_3Br are CH_3CN + Br, and CH_2CN + HCl, respectively. These product distributions directly reflect differences in thermodynamic stability between alternate products, because there are no exceedingly high barriers along the reaction pathways. Halogen abstraction from the fluorinated systems also leads to different final products. In CF_3Cl the most stable product is CF_3CClN, while in the CF_3Br system it is thermodynamically favourable to break the C–Br bond and form CF_3CN + Br.

Despite the encouraging rate constants, the rates of the direct CX_3Y + CN reaction have not been established because of the lack of concentration data for CN radicals in different parts of the atmosphere. The impact of the cyano radical reaction on the stability of halomethanes could increase significantly if any product species participate in further breakdown reactions. In case the initial reaction does not proceed beyond formation of halogen or hydrogen cyanide, several mechanisms can be imagined that lead to regeneration of the cyano radical, see Figure 6. Photodissociation of ClCN and BrCN occur from excitations into the A band, which is at 202 nm for BrCN and 178 nm for ClCN.[27] These photochemical reactions regenerate CN, which could react with a second halomethane. These wavelengths are in a close to those for photodissociation of HCN,[23] and should therefore reach similar regions of the atmosphere. The released halogen radical could then potentially react with HCN to form an additional CN radical. However, modelling shows that the Cl + HCN → HCl + CN reaction has a very low rate constant (k=10^{-11} s^1M^{-1}) compared to the primary CX_3Y + CN reactions (k=10^1-10^9 s^1M^{-1}), and would not regenerate CN radicals in any significant quantities.

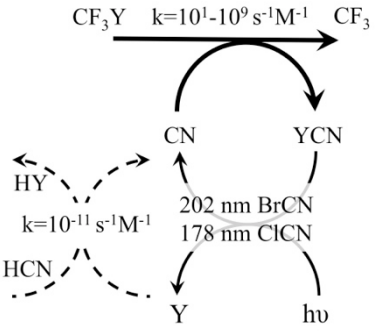

Figure 6. Possible reaction cycles for the regeneration of cyano radicals

Conclusion

The AFIR algorithm has been used to automatically locate the stationary points of the bimolecular reactions between haloalkanes CX_3Y (X=H,F Y=Cl,Br) and ground state ($^2\Sigma^+$) cyano radicals. Between eight and eleven pathways have been identified for each system. Many of them lead to further reactions, and the potential energy surface for e.g., CH_3Cl + CN has 71 different stationary points. Parts of this complexity can be removed by discriminating between mechanisms based on the relative reaction rates in the entrance channel. In most cases the differences in barrier heights, calculated using the accurate G4 method, are much larger than the expected errors of the method, which increases the reliability of the conclusions.

For CH_3Cl + CN the highest rate constant (10^8 s^1M^{-1}) is obtained for hydrogen abstraction, in full agreement with experiment. Replacing chlorine for bromine in CH_3Br lowers the halogen abstraction barrier significantly and gives essentially the same rate constants for hydrogen and halogen abstraction (10^9 s^1M^{-1}). Replacing hydrogen with fluorine leads to lower reaction rates as it not only eliminates hydrogen abstraction, but also decreases the rate constants for halogen abstraction, from 10^4 s^1M^{-1} to 10^1 s^1M^{-1} in CF_3Cl, and from 10^9 s^1M^{-1} to 10^8 s^1M^{-1} in CF_3Br. Fluorine substitution increases the carbon-halogen bond strength because the contributions from the fluorine 2p orbitals stabilize the highest occupied a_1 orbital. At the same time, the Cl/Br contributions to the frontier orbital decrease. The smaller overlap and larger energy difference compared to the CN LUMO increase the energy barrier. Most of the trends for the rate constants follow chemical intuition, but the differences in rate constants have not been previously quantified.

Accurate calculations of product distributions require detailed descriptions of the reaction dynamics, especially for the intermediates formed after the initial abstraction reaction, e.g., CH_2Cl + HCN in the chloromethane system. Although the ratio between product dissociation and radical rebound mechanism cannot be calculated from the AFIR results, the detailed explorations of the potential energy surfaces form the bases for more detailed description of the reaction dynamics.

Independent of the rates for the reactions with cyano radicals, the results highlight the enormous potential of the AFIR method in the analysis of complex chemical reactions. In this work the method has identified a large number of mechanism for breakdown of halomethanes using cyano radicals that have not been previously, neither theoretically nor experimentally, known. These predictions can be tested e.g., using a crossed molecular beam approach, to probe the different decay rates of cyano radicals and to identify the different reaction products. The encouraging rate constants motivate future studies of other radical species.

Computational details

The stationary points of the CX_3Y + CN potential energy surfaces were located using the AFIR algorithm,[5-6] implemented in a local development version of the Global Reaction Route Mapping (GRRM) program. The AFIR method systematically explores the potential energy surface, starting from a random orientation and position of the reactant molecules. It has successfully been applied e.g., to the reaction between vinyl alcohol and formaldehyde,[5] $HCo(CO)_3$-catalyzed hydroformylation,[6a] and the enzymatic mechanism of isopenicillin N synthase (IPNS),[6b] The method has recently been extended also to intramolecular pathways.[28] The detailed steps of the AFIR method can be found in reference [5].

Electronic structure calculations were performed with the Gaussian09 program.[29] Geometries are optimized using the B3LYP functional and the GTBas3 basis set. This basis set is equal to 6-31g(2df,p) for H, C, N, F, and Cl, and 6-31G(2fg) for Br. Details of the AFIR reaction path search are given in the Supporting Information. AFIR explorations were performed independently for CH_3Cl and CF_3Cl. For CH_3Cl, the AFIR search resulted in 35 local minima and 36 TS structures, but only those structures that lead forward to new products are presented here. For CF_3Cl, where the search focused only on low- energy pathways, the result was 18 local minima and 13 TS structures. All AFIR paths have been confirmed by intrinsic reaction coordinate calculations connecting the TS with corresponding minima. Stationary points for CH_3Br and CF_3Br were located from their chlorine-containing counterparts. Geometries with weakly interacting fragments were re-optimized using the ultrafine grid and tight convergence criteria for geometry optimization in Gaussian09. All minima have zero imaginary frequencies, and all TS structures have a single imaginary frequency.

Relative free energies are calculated using the composite G4 method and reported compared to the separated CX_3Y + CN reactants. This method employs structures optimized at B3LYP/GTBas3 level of theory, but calculates energies at the CCSD(T)/6-31G(d) level of theory with corrections for basis set incompleteness at MP4, MP2 and HF levels of theory.[7] Zero-point vibrational energy and thermal corrections to the free energy at 298.15 K are obtained from the B3LYP/GTBas3 frequencies, scaled by a factor of 0.9854. G4 is a highly accurate method with a mean unsigned difference (MUD) of 0.83 kcal/mol for the 454 entries in the G3/05 benchmark set.[7] The cyano radical is difficult to treat accurately due to a large amount of spin contamination,[30] but the G4 method calculates the enthalpy of formation of CN and HCN with errors of only -0.82 and 0.87 kcal/mol respectively. The errors in enthalpy of formation for the halomethanes are all <0.4 kcal/mol.[31]

The G4 method also performs well for reaction barriers with a MUD of 0.91 kcal/mol and a maximum error of 2.39 kcal/mol for the 38 barriers in the hydrogen transfer barriers height (HTBH) data set.[20] The errors are larger for the non-hydrogen transfer barrier height (NHTBH) data set, 1.81 kcal/mol MUD and 8.48 kcal/mol maximum deviation. The larger errors are mainly due to deficiencies in the B3LYP/GTBas3 geometries, e.g., for some fluorine-containing systems, and significantly lower errors were obtained when using QCISD/MG3 geometries (0.47 kcal/mol MUD and 1.93 kcal/mol maximum).[20, 32] As the relative energies of the transition states in the entrance channels are critical in the present study, all pathways with barriers within 10 kcal/mol of the lowest TS, i.e., TS 0, TS 3, and TS 8 for CH_3Y as well as TS 1 for CF_3Y, were therefore re-optimized using QCISD/GTBas3. The reported free energies for these stationary points also include free-energy corrections from QCISD/GTBas3 instead of B3LYP/GTBas3. Although GTBas3 (double-ζ) is a smaller basis set than MG3 (triple-ζ), the maximum errors in calculated barrier heights with the modified G4 method are still expected to be around 2 kcal/mol.

To test the stability of the results, single-point energy calculations were performed for all stationary points using CCSD(T) as well as the density functionals B3LYP[33] and M06-2X,[34] in all three cases with the aug-cc-pvtz basis set. Compared to G4, B3LYP underestimates the reaction barriers with a

mean signed difference (MSD) of -7.1 kcal/mol and a MUD of 7.1 kcal/mol. The deviations were larger for CF_3Y systems (MUD of 8.9 kcal/mol) than for CH_3Y systems (5.3 kcal/mol). The mean differences were much smaller for M06-2X, -3.4 kcal/mol MSD and 3.4 kcal/mol MUD, and the error did not increase for the fluorine-containing systems. Finally, CCSD(T) gave similar results to the G4 calculations with a MUD of 1.3 kcal/mol. Due to the similarity in the relative energies, the analysis of molecular properties are performed using the CCSD/aug-cc-pvtz generalized density. The exception is CN for which the analysis of the β LUMO composition is done with restricted open shell (RO) M062X as the RO-CCSD generalized density is not available. The properties of the CN radical have also been calculated using CASSCF(9,8), i.e., nine electrons in eight orbitals.

Second-order rate constants have been calculated with the Polyrate program,[35] using conventional transition state theory (TST) at 298.15 K with Wigner corrections for tunnelling. Free-energy barriers ($\Delta G^{\ddagger}$) for the TST calculations and imaginary frequencies (ν_i) for the tunnelling corrections are taken from the modified G4 method. Activation energies (E_a) for the bimolecular reactions are calculated relative to the preceding reactant complex using $E_a=\Delta H^{\ddagger}+2RT$.

Tests with canonical variational theory (CVT) and zero-curvature tunnelling (ZCT), at either M062X/GTBas3 or B3LYP/GTBas3 levels, did not affect rate constants by more than a factor of ten. However, these calculations could not be properly converged for all systems, which prevented the use of higher levels of theory. A possible error of a factor of ten for the rate constants corresponds to an uncertainty in the barrier height of 1.4 kcal/mol. With an estimated error from the electronic structure calculations around 2 kcal/mol, the errors in the effective barrier heights should be 4 kcal/mol or less. In the evaluation of substituent effects, e.g., Cl/Br substitution, similar systematic errors are made and a difference in barrier height of 1 kcal/mol for the same reaction in two different halomethanes has been considered significant.

Acknowledgements

We thank Daniel Roca Sanjuán for help with the Polyrate calculations and Henrik Ottosson for helpful suggestions. ML acknowledges financial support from the Marcus and Amalia Wallenberg Foundation. Parts of the research were funded by the Swedish Research Council. The computations were performed on resources provided by SNIC through Uppsala Multidisciplinary Center for Advanced Computational Science (UPPMAX) under project p2011004.

Keywords: Gas-phase reactions • Quantum Chemistry • Radical reactions • Reaction mechanisms • Transition states

[1] a) M. Molina, F. Rowland, *Nature* **1974**, *249*, 810-812; b) F. Rowland, M. J. Molina, *Rev. Geophys. Space Ge.* **1975**, *13*, 1-35; c) J. G. Anderson, D. Toohey, W. Brune, *Science* **1991**, *251*, 39-46.
[2] J. A. Kaye, S. A. Penkett, F. M. Ormond, P. Fraser, D. Fisher, P. Bloomfield, S. Sander, M. Ko, NASA Reference Publication 1339, **1994**.
[3] a) K. Tanaka, T. Hisanaga, *Sol. Energy* **1994**, *52*, 447-450; b) H. M. Cheung, S. Kurup, *Environ. Sci. Technol.* **1994**, *28*, 1619-1622; c) C. P. Grey, D. R. Corbin, *J. Phys. Chem.* **1995**, *99*, 16821-16823; d) W.-k. Chang, C. S. Criddle, *Biodegradation* **1995**, *6*, 1-9; e) J. Burdeniuc, R. H. Crabtree, *Science* **1996**, *271*, 340-341; f) W. Choi, M. R. Hoffmann, *Environ. Sci. Technol.* **1997**, *31*, 89-95; gH.-M. Hung, M. R. Hoffmann, *J. Phys. Chem. A* **1999**, *103*, 2734-2739.
[4] R. von Glasow, P. J. Crutzen, in *Treatise on Geochemistry, Vol. 4* (Ed.: R. F. Keeling), Elsevier-Pergamon, Oxford, **2007**, pp. 1-67.
[5] S. Maeda, K. Morokuma, *J. Chem. Theory Comput.* **2011**, *7*, 2335-2345.
[6] a) S. Maeda, K. Morokuma, *J. Chem. Theory Comput.* **2012**, *8*, 380-385; b) S. Maeda, E. Abe, M. Hatanaka, T. Taketsugu, K. Morokuma, *J. Chem. Theory Comput.* **2012**, *8*, 5058-5063.
[7] L. A. Curtiss, P. C. Redfern, K. Raghavachari, *J. Chem. Phys.* **2007**, *126*, 084108.
[8] G. W. Gribble, *Acc. Chem. Res.* **1998**, *31*, 141-152.
[9] D. Yang, M. Lin, in *The Chemical Dynamics Kinetics of Small Radicals* (Eds.: K. Liu, A. Wagner), World Scientific, River Edge, **1996**, pp. 164-213.
[10] R. Cicerone, R. Zellner, *J. Geophys. Res.-Oceans* **1983**, *88*, 10689-10696.
[11] a) N. Balucani, O. Asvany, L. Huang, Y. Lee, R. Kaiser, Y. Osamura, H. Bettinger, *Astrophys. J.* **2000**, *545*, 892; b) N. Balucani, O. Asvany, A. Chang, S. Lin, Y. Lee, R. Kaiser, Y. Osamura, *J. Chem. Phys.* **2000**, *113*, 8643; c) R. I. Kaiser, N. Balucani, *Acc. Chem. Res.* **2001**, *34*, 699-706; d) P. Casavecchia, N. Balucani, L. Cartechini, G. Capozza, A. Bergeat, G. G. Volpi, *Faraday Discuss.* **2002**, *119*, 27-49; e) N. Choi, M. Blitz, K. McKee, M. Pilling, P. Seakins, *Chem. Phys. Lett.* **2004**, *384*, 68-72; f) K. L. Gannon, D. R. Glowacki, M. A. Blitz, K. J. Hughes, M. J. Pilling, P. W. Seakins, *J. Phys. Chem. A* **2007**, *111*, 6679-6692; g) A. J. Trevitt, F. Goulay, G. Meloni, D. L. Osborn, C. A. Taatjes, S. R. Leone, *Int. J. Mass Spectrom.* **2009**, *280*, 113-118; h) F. Leonori, K. M. Hickson, S. D. Le Picard, X. Wang, R. Petrucci, P. Foggi, N. Balucani, P. Casavecchia, *Mol. Phys.* **2010**, *108*, 1097-1113.
[12] F. Leonori, R. Petrucci, X. Wang, P. Casavecchia, N. Balucani, *Chem. Phys. Lett.* **2012**, *553*, 1-5.
[13] A. D. Estillore, L. M. Visger, R. I. Kaiser, A. G. Suits, *J. Phys. Chem. Lett.* **2010**, *1*, 2417-2421.
[14] S. B. Morales, C. J. Bennett, S. D. Le Picard, A. Canosa, I. R. Sims, B. Sun, P. Chen, A. H. Chang, V. V. Kislov, A. M. Mebel, *Astrophys. J.* **2011**, *742*, 26.
[15] A. J. Trevitt, S. Soorkia, J. D. Savee, T. S. Selby, D. L. Osborn, C. A. Taatjes, S. R. Leone, *J. Phys. Chem. A* **2011**, *115*, 13467-13473.
[16] a) L. R. Copeland, F. Mohammad, M. Zahedi, D. H. Volman, W. M. Jackson, *J. Chem. Phys.* **1992**, *96*, 5817; b) C. Huang, W. Li, A. D. Estillore, A. G. Suits, *J. Chem. Phys.* **2008**, *129*, 074301.
[17] a) I. R. Sims, J.-L. Queffelec, D. Travers, B. R. Rowe, L. B. Herbert, J. Karthäuser, I. W. Smith, *Chem. Phys. Lett.* **1993**, *211*, 461-468; b) D. Yang, T. Yu, M. Lin, C. Melius, *Chem. Phys.* **1993**, *177*, 271-280; c) G. Bethardy, F. Northrup, R. G. Macdonald, *J. Chem. Phys.* **1996**, *105*, 4533.
[18] V. Samant, J. F. Hershberger, *Chem. Phys. Lett.* **2008**, *460*, 64-67.
[19] a) A. C. Crowther, S. L. Carrier, T. J. Preston, F. F. Crim, *J. Phys. Chem. A* **2008**, *112*, 12081-12089; b) V. R. Morris, F. Mohammad, L. Valdry, W. M. Jackson, *Chem. Phys. Lett.* **1994**, *220*, 448-454.
[20] L. A. Curtiss, P. C. Redfern, K. Raghavachari, *Chem. Phys. Lett.* **2010**, *499*, 168-172.
[21] R. A. Rose, S. J. Greaves, T. A. Oliver, I. P. Clark, G. M. Greetham, A. W. Parker, M. Towrie, A. J. Orr-Ewing, *J. Chem. Phys.* **2011**, *134*, 244503.
[22] P. Metrangolo, F. Meyer, T. Pilati, G. Resnati, G. Terraneo, *Angew. Chem., Int. Ed.* **2008**, *47*, 6114-6127.
[23] J. Guo, R. Eng, T. Carrington, S. Filseth, *J. Chem. Phys.* **2000**, *112*, 8904-8909.
[24] R. Thomson, F. Dalby, *Can. J. Phys.* **1968**, *46*, 2815-2819.
[25] a) S. Shaik, A. Shurki, *Angew. Chem. Int. Ed* **1999**, *38*, 586-625; b) S. Shaik, P. C. Hiberty, *Rev. Comp. Chem.* **2004**, *20*, 1-87.
[26] P. Staneke, J. Kauw, M. Born, N. Nibbering, *Rapid Commun. Mass Spectrom.* **1997**, *11*, 124-132.
[27] W. Felps, K. Rupnik, S. P. McGlynn, *J. Phys. Chem.* **1991**, *95*, 639-656.
[28] S. Maeda, T. Taketsugu, K. Morokuma, *J. Comput. Chem.* **2014**, *35*, 166-173.
[29] M. J. Frisch, G. W. Trucks, H. B. Schlegel, G. E. Scuseria, M. A. Robb, J. R. Cheeseman, G. Scalmani, V. Barone, B. Mennucci, G. A. Petersson, H. Nakatsuji, M. Caricato, X. Li, H. P. Hratchian, A. F. Izmaylov, J. Bloino, G. Zheng, J. L. Sonnenberg, M. Hada, M. Ehara, K. Toyota, R. Fukuda, J. Hasegawa, M. Ishida, T. Nakajima, Y. Honda, O. Kitao, H. Nakai, T. Vreven, J. A. Montgomery Jr., J. E. Peralta, F. Ogliaro, M. J. Bearpark, J. Heyd, E. N. Brothers, K. N. Kudin, V. N. Staroverov, R. Kobayashi, J. Normand, K. Raghavachari, A. P. Rendell, J. C. Burant, S. S. Iyengar, J. Tomasi, M. Cossi, N. Rega, N. J. Millam, M. Klene, J. E. Knox, J. B. Cross, V. Bakken, C. Adamo, J. Jaramillo, R. Gomperts, R. E. Stratmann, O. Yazyev, A. J. Austin, R. Cammi, C. Pomelli, J. W. Ochterski, R. L. Martin, K. Morokuma, V. G. Zakrzewski, G. A. Voth, P. Salvador, J. J. Dannenberg, S. Dapprich, A. D. Daniels, Ö. Farkas, J. B. Foresman, J. V. Ortiz, J. Cioslowski, D. J. Fox, Gaussian, Inc., Wallingford, CT, USA, **2009**.
[30] M. Urban, J. D. Watts, R. J. Bartlett, *Int. J. Quantum Chem.* **1994**, *52*, 211-225.
[31] http://www.cse.anl.gov/OldCHMwebsiteContent/compmat/g4theory.htm (accessed May 2 2014).
[32] Y. Zhao, N. González-García, D. G. Truhlar, *J. Phys. Chem. A* **2005**, *109*, 2012-2018.
[33] A. D. Becke, *J. Chem. Phys.* **1993**, *98*, 5648-5652.
[34] Y. Zhao, D. G. Truhlar, *Theor. Chem. Acc.* **2008**, *120*, 215-241.

[35] J. Zheng, S. Zhang, B. Lynch, J. Corchado, Y. Chuang, P. Fast, W. Hu, Y. Liu, G. Lynch, K. Nguyen, University of Minnesota, Minneapolis, **2010**.

ARTICLE

This study gives new insight into the stability of halomethanes by exploring their reactions with the cyano radical. With the Artificial Force Induced Reaction (AFIR) algorithm new mechanisms for the breakdown of halomethanes have been found and differences in reactivity between halomethanes can be analysed (see Figure). The detailed potential energy surfaces also point the way for better descriptions of the reaction dynamics.

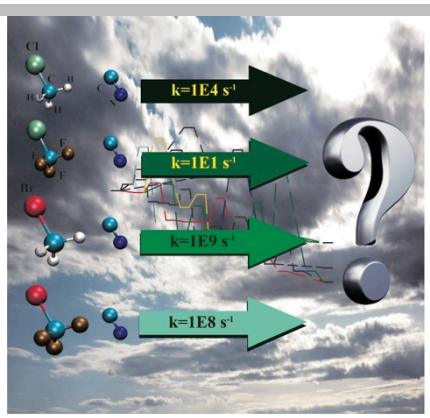

*P. Farahani, S. Maeda, J.S. Francisco, M. Lundberg**

Page No. – Page No.

Complete pathways